IHJPAS. 37 (1) 2024
Ibn Al-Haitham Journal for Pure and Applied Sciences
Journal homepage: jih.uobaghdad.edu.iq
PISSN: 1609-4042, EISSN: 2521-3407

Theoretical Study of the Lasing Output for a Quasi-Three-Level Operation in Nd $^{3+}$:YAG Thin- Disk Laser

[1]Manahil Ameen Mahammed* **[2]Mudhir Shihab Ahmed**

[1,2]Department of Physics, College of Education for Sciences Ibn-AL-Haitham, University of Baghdad, Baghdad, Iraq.

*Corresponding Author. Manahel.ameen2104m@ihcoedu.uobaghdad.edu.iq

Received: 20 March 2023, Received 15 April 2023, Accepted 3 May 2023, Published 20 January 2024

doi.org/10.30526/37.1.3353

Abstract

In this research, the effect of each of the concentrations (Nd^{+3}) was studied (N) the thickness of the thin disk (d) the number of times that the pumping beam passes through the effective medium of this laser (M_p) the reflectivity of the laser output mirror ($R_{2)}$ The losses of the effective medium (L) and the pumping power used in achieving the reverse qualification (P_P) on each of the pumping threshold capacities ($P_{p.th}$) and the output power of the laser (P_{out}) and the efficiency (ŋ) in Nd^{3+} thin-disk lasers (TDLs) pumping quasi-three-level With continuous operation (cw), at room temperature, and in the Gaussian mode (TEM00),

We found under these operating conditions for this laser design that each of the (P_{out}) and (ŋ) increases by increasing each of (N), (d), (M_P), and (R_2), while the ($p_{p.th}$) decreases with this increase. We also found that as the losses (L) increases (p_{out}) and (ŋ) decrease, and ($p_{p.th}$) increase, as for increasing the pumping capacity, it leads to an increase in (P_{out}) only. Both (P_{out}) and (ŋ) are not affected by such an increase. In light of these results, the typical values for these coefficients were determined, and then you get the highest value for p_{out} and (ŋ) the lowest value for ($p_{p.th}$) for this laser design under the operating conditions that were adopted in this research.

Keywords: thin- disk laser, continuous wave operation, single mode laser, typical values.

1. Introduction

The mechanism represents the improvement of detail by strong lasers to higher efficiencies, as they are constrained by the warm waste generated in the laser medium. The warmth of the waste leads to a temperature slope and thermal-optical aberrations, which completely limit the natural illumination and power of powerful detail lasers.Quasi-three-level lasers display a limited quantity of quantum deformities and low nonradioactive energy movement; however, they should be siphoned hard to get productive laser outflow at room temperature [1]. The meager circle-molded (Nd^{3+}:YAG) component is patched on the warmth sink and depends on exceptionally effective warmth expulsion because of the small thickness of the gem. To build

siphon retention proficiency, different siphon plans, for example, the sing allegorical multi-pass siphoning structure [1, 2],

A gem plate with a thickness more modest than the breadth of the circle is mounted with one of its faces, which is high-reflectivity covered for both the laser and the siphon frequency, on a warmth sink. Diode-siphoned slender plate lasers (TDL) all the while give high power, high optical proficiency, and great pillar quality. The significant utilizations of TDL are cutting, welding, far-off welding, and half-breed welding [1, 2]. In a powerful system, a multi-pass framework along with a diode laser is utilized to siphon a few hundred micrometers thick. The multi-pass framework is used for expanding siphon laser assimilation. Such conditions bring about the improvement of the siphon pillar profile on the plate surface, which thusly brings about better execution of the TDL [2].

There is an uncommon kind of framework that can be viewed as a moderate between the three-level and the four-level frameworks. This happens when the lower laser level is near the ground level. The population is dispersed into levels as indicated by Boltzmann's constant, so in warm balance at room temperature T, the energy contrast (ΔE) between those two levels complies ($\Delta E \approx kT$), where k is Boltzmann's constant. In these conditions, the lower laser level will be populated, affecting the light intensification measure. [3]

2. Analytical solution:

2.1. Boltzmann occupation factors

A solid-state laser's gain material is made up of a host material, such as glass or crystal that has been doped with optically active ions. Related energy levels determine stimulants and the spectroscopic characteristics of the gain material.

The energy between the nucleus and the electrons, the Coulomb interaction, and the spin-orbit interaction all play a big role in selecting such energy levels. According to the Stark effect's definition [4], this divides energy levels into multiples of Stark, each of which might include numerous Stark levels. When the separate Stark levels are coupled by the phonons, the thermal equilibrium of the energy levels is achieved. Different laser methods can be used depending on the energy splitting [5, 9, and 10].

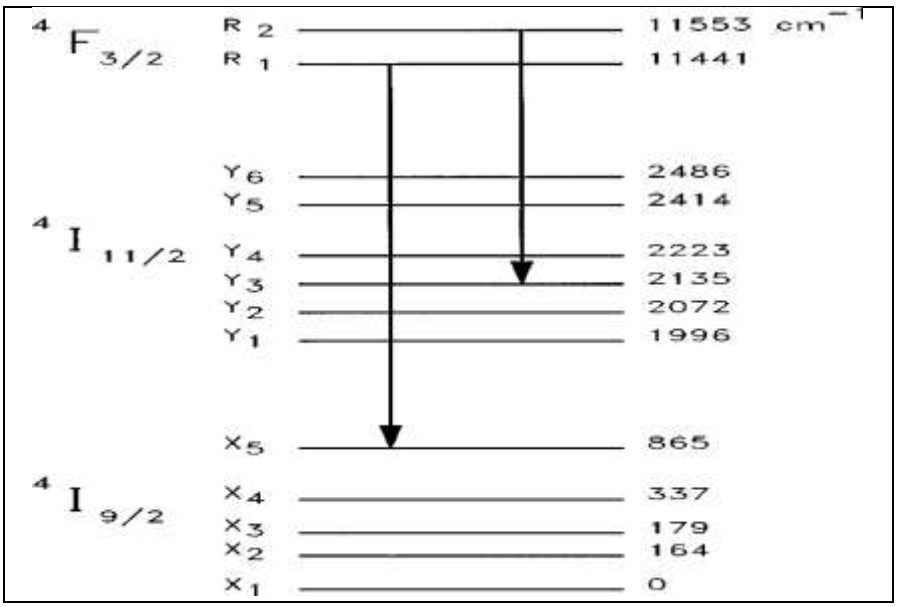

Figure 1. Energy Sublevels distribution of Nd^{3+}:YAG (TDLs)

$$A=KT=209cm^{-1} \quad (1)$$

$$B_1=e^{(-\frac{E_{10}}{A})}+e^{(-\frac{E_{11}}{A})}+e^{(-\frac{E_{12}}{A})}+e^{(-\frac{E_{13}}{A})}+e^{(-\frac{E_{14}}{A})} \quad (2)$$

$$B_2=e^{(-\frac{E_{21}}{A})}+e^{(-\frac{E_{22}}{A})}+e^{(-\frac{E_{23}}{A})}+e^{(-\frac{E_{24}}{A})}+e^{(-\frac{E_{25}}{A})}+e^{(-\frac{E_{26}}{A})} \quad (3)$$

$$B_3=e^{(-\frac{E_{31}}{A})}+e^{(-\frac{E_{32}}{A})} \quad (4)$$

$$B_4=e^{(-\frac{E_{41}}{A})}+e^{(-\frac{E_{42}}{A})} \quad (5)$$

$$f_l^{808nm}=e^{(-\frac{E_{10}}{A})}/B_1 \quad (6)$$

$$f_u^{808nm}=e^{(-\frac{E_{41}}{A})}/B_4 \quad (7)$$

$$f_l^{946nm}=e^{(-\frac{E_{14}}{A})})/B_1 \quad (8)$$

$$f_u^{946nm}=e^{(-\frac{E_{31}}{A})}/B_3 \quad (9)$$

2.2. Beam quality aspects

The beam quality represented by the times diffraction-limit factor (M^2), which is evaluated using a coherent mode master, is dependent on the resonator configuration [6].

The two-mirror resonator used in the resonant cavity has an out-coupling mirror with a curvature radius of (r_1) and a thin disk mirror with a dynamic curvature radius of (R_2) brought on by heating and stress. The equation below shows that (M^2) is considered to be proportional to the pump spot radius, (w_p), and inversely proportional to the thin disk's pump spot radius, (w_f), if (TEM_{00}). [7].

$$M^2=\frac{a\,w_p}{w_f} \quad (10)$$

The constant (a) denotes the overlap between the pumping beam intensity and the lasing mode intensity. The multimode Gaussian beam only takes up about (85%) of the pump spot in reality, according to (TDLs) calculations, even though (a) = (1) if there is perfect overlap. The beam radius over the resonator length is (M^2 = 9.8) for a beam quality number. [8,9,10].

The radius of the laser mode must be tailored to the radius of the pump spot (w_p) for the basic mode operation of TDLs. The spot of pumping serves as a soft aperture due to re-absorption in the thin disk's unpamper portion. For small radii (w_f) of the TEM_{00} mode on the disk, higher-order laser modes can oscillate if their radii are still junior to the radius of the pump spot [11].

These higher-order states can be successfully inhibited by increasing (w_f). If (w_f) becomes too large, the TEM_{00} mode's losses increase as well. For the disks we used, an optimal fundamental mode operation [12]

2.3 Rate equations

The sub-level of the ground state is the lowest laser level, as shown by examining the rate equations for a quasi-three-level laser. In fact, the most significant types of lasers currently in use belong to these two classes of lasers. One can cite a few applications for the four-level laser class as examples: (1) For the majority of the numerous potential transformations, ion crystal lasers, such as neodymium lasers, in a variety of hosts [13]

2.3.1. Quasi-Three-Level Laser

It is assumed that all sub-levels of the ground state are closely connected and in a condition of thermal equilibrium in the semi-three-level laser, where the lower level of the laser is level 1 in **Figure 2**. Similar to the upper laser level, Level 2, which is considered to be in thermal equilibrium because it is a member of a group of upper state sublevels. Hence let's

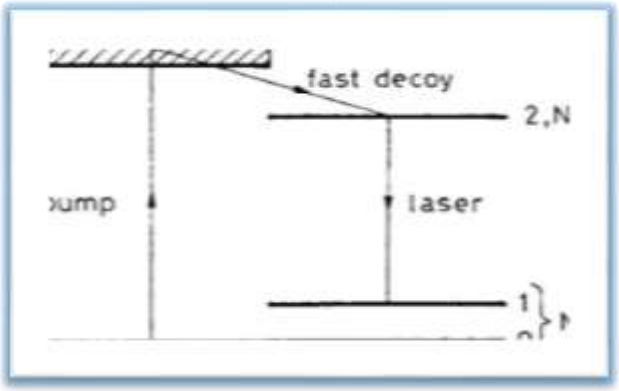

Figure 2. quasi-three-level laser scheme.

N_1 and N_2 be is the combined populations of all ground states and all higher state sublevels. We shall only be interested in populations N1 and N2, as we again assume a very rapid decay from the pump level(s) to the sublevels of the upper state (a quasi-ideal three-level state).

Now let's assume that the energy difference between sublevels 1 and 0 is comparable to kT and that sublevel 0 represents the lowest sublevel of the ground state. Laser photons will be absorbed in regions of the lower laser level where a negligible portion of the ground-state population, N1, is present. The rate equations for each of the lower and upper state laser sublevels can be written in terms of, after the discussion,The relaxation durations for energy levels inside a manifold are quite short due to the small energy splitting of each manifold. The rate equations for the ground state level (E_1) with populations (N), and the excited state level (E_2) with populations (N_u) can be expressed as follows: [9, 10, 13]

$$\frac{dN_2}{dt} = [\sigma_{ap}\,(N - N_u) - \sigma_{ep}\,N_u] * \frac{I_P \eta_a \lambda_p}{\alpha_p dhc} + [\sigma_{al}(N - N_u) - \sigma_{el} N_u * \frac{I_L M_L \lambda_L}{hc} - \frac{N_2}{\tau} \quad (11)$$

$$\frac{dI_L}{dt} = I_L M_L\, d[\sigma_{al+\sigma_{el}})N_u) - \sigma_{aL} N] \frac{c}{2L} * \frac{I_L\, c}{2L}\, [-\ln(1 - T_r) - \ln(1 - L)] \quad (12)$$

λp is the Pumping wavelength, σ_{ap} is Absorption Cross-section of Pumping, σ_{ep} is Stimulated Cross-section of Pumping, λ_L is Lasing wavelength, σ_{aL} is Absorption Cross-sectio of Lasing σ_{el} is Stimulated Cross-section of Lasing, T_r is Transmission of the output coupler, f_l is Thermal Boltzmann factor in lower level, f_u is Thermal Boltzmann factor in upper level, k is Boltzmann's constant, h is Planck's constant, and N_u is the ion concentration in the upper manifold. N is the total ionic concentration, α_p is the assimilation coefficient for siphon radiation, I_P is the average intensity of the pump in the crystal. I_L is the energy intensity of the scattered laser radiation inside the resonator, η_a is Absorption efficiency, M^2 is Quality factor, w_p is Pump radius, w_f is Base Transverse Mode Half Diameter TEM00, $P_{p.th.1}$ is Pump power at threshold, A_p is Effective area of the pumping spot, ν_p is Pump frequency, P_{out} is Laser out power, η is Efficiency of disk laser, M_P is the number of lasers that pass through the crystal for each resonator, τ is Lifetime of the excited state, d is The thickness of the thin disk, c is The velocity of an electromagnetic wave in a vacuum, and T is the temperature of the heat sink.

2.3.2. Steady- State Solution

During steady-state laser operation, the values for dNu/dt and (dI_L/dt) are equal to zero when the system is in an equilibrium state. For the population inversion, it is obtained immediately (Na)

2.3.3. Round-Trip loss

What portion of the laser field's energy is converted to background radiation depends on the round-trip loss or background loss in laser physics. Unusable at each round-trip, it can be absorbed or scattered, the round-trip losses in the resonator can be describe as [14]

$$\delta = -\ln(1 - T_r) - \ln(1 - L) \quad (13)$$

where

$$T_r = 1 - R_2 \quad (14)$$

(R2) is the output reflectivity at laser wavelength for the quasi-three-level system, and (L) is the internal loss at the quasi-three-level system, respectively [4].

2.3.4. Stokes and absorption efficiency

Tthe stokes efficiency is defined as [15]

$$\eta_s = \frac{\lambda_p}{\lambda_l} \quad (15)$$

where (λ_p) is the pumping wavelength and (λ_l) is the laser wavelength at quasi-three-level. However, the absorption efficiency for the absorbed intensity and initial pump intensity in given by using the Beer-Lambert law for multi pass systems[16]

$$\eta_a = R_p\,(1 - (\exp(-M_P * \alpha_p * d)) \quad (16)$$

where.

(R_p) is the total reflectivity of the multi-pass pumping system, and (M_p) is the number of passes of the pump beam in the active medium. The absorption coefficient at the pumping wavelength is given by[14]

$$\alpha_p = \sigma_p f_{Lp} N_t \quad (17)$$

where (f_l^p) is a fractional occupation of density lower pump State However,

the absorption coefficient at laser wavelength is given by

$\alpha_l = \sigma_l f_l^l N_t$ (18)

where (f_l^l) is a fractional occupation of density lower laser state.

2.3.5. Pump Power at the Threshold (P_p.th)

Where the threshold conditions [16]

$Nu = N_{u.th}$ (19)

$I_l = 0$ (20)

$I_p = I_{p.th}$ (21)

$p_{p.th} = I_{p.th} * A_p$ (22)

$A_p = \pi w_p^2$ (23)

Then

$$P_{.P.th} = \frac{\pi hc}{4\sigma_l \eta_p \lambda_p (f_{up}+f_{lp})\tau} * \frac{2\omega_1^2}{1-\exp(\omega_1^2/\omega_2^2)} *(-\ln R_2+L+L_{10}) \quad (24)$$

Here f_u and f_l signify the population numbers in the Stark components of the upper and lower laser levels involved in the 808 nm emission, respectively. p stands for pump quantum efficiency. f_l is the population fraction of the 4F3/2 Stark level employed for the emission at 946 nm. L, are the residual losses on the return trip.

$L_{01} = 4\sigma_l f_l^p N$ (25)

N is the concentration of Nd and is the reabsorption loss for the quasi-three-level emission. R_2 is the reflectivity of output mirror at 946nm.

2.3.6. Laser output power (Pout).

By the steady-state condition and when: [15]

$I_{out} = T_r I_l$ (26)

$P_p = A_p I_p$ (27)

$P_{out} = A_p I_{out}$ (28)

The formula of equation output power is given by [16]

$$P_{out} = \frac{Tr}{(-(1-Tr)-ln(1-L))} \eta_a \eta_s (P_p - P_{P.th}) \quad (29)$$

2.3.7. Efficiency(ŋ)

For any Laser design, the equation of the output Power is given by [17]

$P_{out} = \eta (P_p - P_{P.th.})$ (30)

From combining Eq. (29) and Eq. (30), the equation of efficiency (Ƞ) is obtained by

$$\eta = \frac{T_r}{-\ln(1-T_r)-\ln(1-L)} \eta_a \eta_s \quad (31)$$

3. Numerical solution

In this article, the MATLAB program was used to find the numerical solution to each of the $P_{p.th}$ equations with the number (24) and the equation P_{out} with the number (29) and the equation (ŋ) with the number (31). **Figure (1)** shows the values of energies for all levels produced by the stock effect of the Nd^{3+} element in the YAG crystal, which are necessary to calculate the Boltzmann coefficients at low and high room temperature, which are shown in **Figure (2).**

Table 2 shows the values of these coefficients at the pumping wavelength (808 $*10^{-9}$ m), which were calculated through the two equations (6) and (7), respectively. These coefficients were calculated at the laser wavelength (946$*10^{-9}$ m), which were calculated through equations (8) and (9), respectively. As for the value of (M^2), which was calculated through the equation (10), the

arameters	Value	unit
Hosts	YAG	-
λ_p	$808*10^{-9}$	m
σ_p	$7.9*10^{-24}$	m
λ_l (Q.3l)	$946*10^{-9}$	m
σ_l (Q.3l)	$3.7*10^{-24}$	m^{-2}
τ	$230*10^{-6}$	sec
T	300.15	k^o
a	0.85	-
w_p	0.77	-
w_0	$195*10^{-6}$	m
w_1	$229.42*10^{-6}$	m
w_3	$250*10^{-6}$	m
h	$6.6205*10^{-34}$	J.sec
k	$1.38*10^{-23}$	$J.c/K^o$
c	$3*10^8$	m/sec

value of (w_P =229.42 $*10^{-6}$) was adopted in order to obtain (M^2 = 1) to ensure that the laser in question works in the basic transverse pattern (TEM_{00}).

Table 2. Boltzmann coefficients for Nd^{+3}:YAG thin disk laser for quasi-three-level

Parameters	Value
f_l (808)	0.4634
f_u (808)	0.9045
f_l (946)	0.0079
F_u (946)	0.5991

Table (3) shows all the values of the equations needed to solve the above equations using MATLAB. These values were chosen from recently published international research on the laser in question. Through this, the effect of the factors affecting the operation of this laser design was studied, as follows:

Table.3 Parameters needed to obtain the numerical solution by MATLAB program for Nd^{3+}:YAG (TDLs)

3.1. Effect of Concentration (n)

Figure 3 clarifies the relationship of the laser output capacity with the three pumping capacity values for concentration (n), where we note that both the ability of the laser output and efficiency are higher when focused (at 1.1%), while the pumping threshold capacity is less valuable to it at this focus, and this is what is indicated by **Table 3.** We also noticed that increasing the focus beyond these values did not change much in its values, both in terms of the ability of the laser output and efficiency.

It is preferable when using the Nd^{3+} element to work with relatively low concentrations compared to the Yb^{3+} element because the time for the atoms to reach the upper laser level will

decrease with an increase in the focus of the Nd^{3+} element, which causes an increase in the capacity threshold.

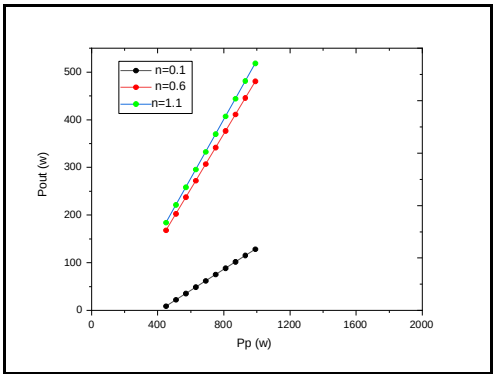

Figure 3. output power versus pumping power at different values of concentration (N)

Table 3. pumping power and efficiency at different values of concentration (n)

Parameters	N at %			
	0.1	0.6	1.1	
Ŋ(946)%	22.14	57.91	61.92	-
$P_{p.th}$ (946)%	410.3924	160.1204	152.7960	w

3.2. Effect of Thickness (d):

Figure (4) clarifies a relationship that the laser output is with the ability of pumping for three values for fish (d), where we note that both the ability of the laser output and the efficiency are higher when ($d=300*10^{-6}m$) because the fish cushion leads to an increase in both (η_a) and increasing the size of the region from the effective medium to display it directly to the pumping package, and at these values for (d) the ability of pumping is less possible and this is what Table (4) shows and this fish ($d=300*10^{-6}m$) is used globally in a manufacturing. These lasers:

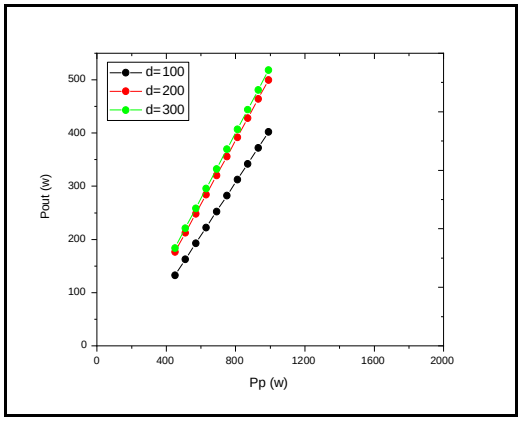

Figure 4. output power versus pumping power at different values of thickness(d)

Table 4. pumping power and efficiency at different values of thickness (d)

Parameters	d (m)			
	$100*10^{-6}$	$200*10^{-6}$	$300*10^{-6}$	Unit
Ŋ(946)%	49.89	59.91	61.92	-
Pp.th (946)%	184.1023	155.6250	152.7960	w

3.3. Effect of output reflectivity (R_2)

Figure (5) explains the relationship of the ability of the laser output to the ability of pumping for three values of reflexes, the laser output, where we note that both the ability of the laser output and the efficiency are higher at (R_2= 0.9). To increase the capacity of the pumping threshold, which negatively affects both the ability of the laser output and efficiency, it is scientifically preferable to be the reflection of the laser output mirror within these limits.

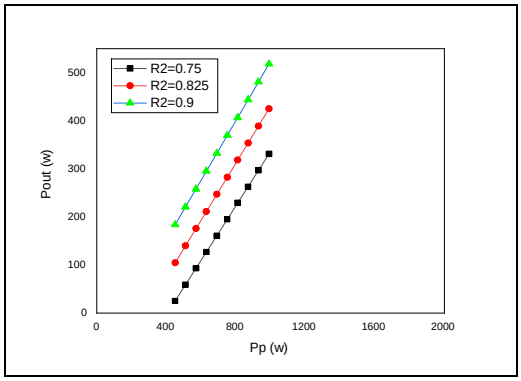

Figure 5. output power versus pumping power at different values of output reflectivity (R_2)

Table 5. pumping power and efficiency at different values of output reflectivity (R_2)

Parameter	R_2		
	0.7	0.825	0.9
Ŋ(946)%	54.87	58.47	61.92
Pp.th (946)%	501.3506	316.1524	28.2412

3.4. Effect of power pumping (Pp)

Forms (6, 7, 8) relationship clarify the leaner output with the ability to pump in the medium, medium, high, consecutive, consecutive views, where we are updated that the liability of the laser output increases by increasing the pumping capacity always because increasing the pumping capacity caused the reverse rehabilitation such as this laser design and thus increasing the number of photons that cause stimulating emission, which is the basis of laser emissions, while you find that everyone who has pumping and efficiency is never affected by this increase.

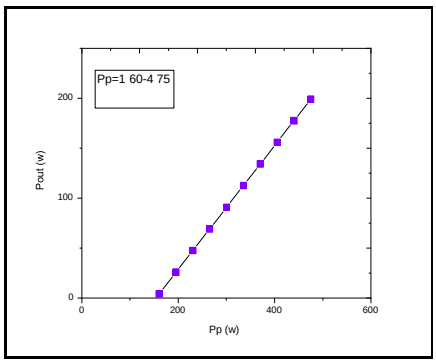

Figure 6. Relationship of laser output power to pumping power in low- range

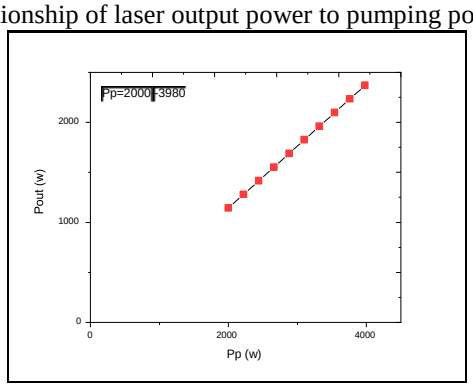

Figure 7. Relationship of Laser Output Power to Pumping Power in Mid-range

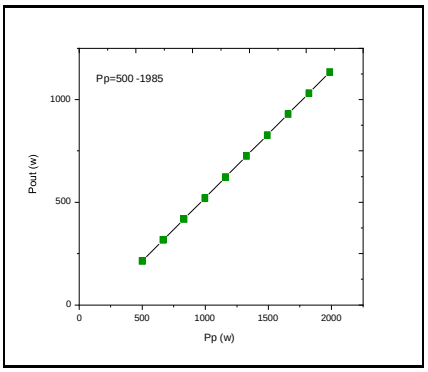

Figure 8. Relationship of laser output power to high- range pumping power

Table (6) shows the optimal values of these factors, which, when used, give us a high exit and efficiency. In addition to that, the pumping capacity is at its lowest value, as with these values, so it is preferable to manufacture this laser in practice according to these optimal values.

Table 6. Typical values of Nd^{3+}:YAG

Parameters	Value	unit
T	300.15	K°
N	1.1 at %	-
d	$300*10^{-6}$	m
M_p	32	-
R_2	0.9	-
L	0	-
λ_p	$808*10^{-9}$	m
λ_1	$946*10^{-9}$	m
w_f	$195*10^{-6}$	m
w_p	$229.42*10^{-6}$	m
w_1	$1170*10^{-6}$	m
w_2	$900*10^{-6}$	m
w_3	$900*10^{-6}$	m
P_p	(160-4000)	w

4. Conclusions

The laser output power (P_{out}) and the efficiency of this laser design (ŋ) increase with the increase of (N),(d), (M_p), and (R_2) in this operating system., While the pumping threshold power ($P_{p.th\ 1,2}$) decreases with the increase of (N), (d), (M_P), and (R_2). - The laser output power (P_{out}) and efficiency (ŋ) decrease while the pumping threshold ($P_{P.th1,2}$) increases with the increase of (L).

Acknowledgement

I extend my thanks to the College of Education for pure science Ibn Al-Haitham, University of Baghdad for providing assistance to complete this work by opening private laboratories and providing scientific facilities by the staff of the Physics Department to help support the research project.

Conflict of Interest

The authors declare that they have no conflicts of interest

Funding: None.

References

1. Karszewski, K. M.; Stewen, C.; Giesen A.; Huge, H.; Theoretical modeling and experimental investigations of the diode-pumped thin-disk Yb :YAG laser, Quantum Electron **1999**,*29*,8 ,697
2. Mohammad ,H. S.; Determination and suppression of back reflected pump power in Yb:YAG thin-disk laser , *Optical Engineer* **2017** ,*56(2)* ,026109-1-8,
3. Hariton, V.; Feasibility study and simulation of a high energy diode pumped solid-state amplifier ,*Tecnico Lisboa*. **2016**,1-94 ,
4. Kazemi, S. S., Mahdieh, M. H.; Determination and suppression of back-reflected pump power in Yb:YAG thin-disk laser, *Optical Engineering* **2017**, *56(2)*, 026109. doi: 10.1117/1.oe.56.2.026109
5. Weichelt, V.; Von, B.; Experimental Investigations on Power Scaling of High-Brightness cw Ytterbium-Doped Thin-Disk Lasers, (July) **2021**, 1–23.
6. Stewen, V.; M.ovlarion, A,; Yb:YAG thin disk laser with 1 kW output power. *optical Society of America.* **2000**, *22*, 13-23

7. Zin, H. L.; Heat generation in quasi-three-level Yb : YAG thin disk lasers, *Optical Society of America* **2017**, *34(8)*, 1669–1676. doi: 10.1364/JOSAB.34.001669.
8. Liu, R.; Research on the adjusting technology of the thin disk laser, *Optik* **2018**, *157*, 400–405. doi: 10.1016/j.ijleo.2017.11.072.
9. Mohammed, A. M.; Mudhir, S. a.; Raed, M. S.; Numerical Analysis of a Lasing Output for the Quasi- Three Level Thin Disk Lasers, *Ibn Al-Haitham International Conference for Pure and Applied Sciences (IHICPS) Journal of Physics* **2021**. Conference Series 1879 32116 doi:10.1088/1742-6596/1879/3/032116
10. Mustafa, M. M.; Mudhir, S. A.; Theoretical Investigations of High Power Yb3+: YAG Thin-Disk Laser, *Ibn Al Haitham Journal for Pure and Applied Science* **2022,** Doi:10.30526/35.4.2854 IHJPAS. 35(4)
11. Mende, J.; Concept of neutral gain modules for power scaling of thin-disk lasers , Applied Physics B*: Lasers and Optics* **2009**, *97(2)*, 307–315. doi: 10.1007/s00340-009-3726-2
12. Peng, Y. H.; High brightness continuous wave ceramic Yb:LuAG thin-disk laser,Optics Express **2015**, *23(15)*, 19618. doi: 10.1364/oe.23.019618
13. Orazio, S.; Principles of Lasers, 5th ed. c *Springer Science Business Media*, LLC **2010**, DOI 10.1007/978-1-4419-1302-9
14. Zhao, W.; Numerical analysis of a multi-pass pumping Yb:YAG thick-disk laser with minimal heat generation , *Applied Optics* **2018**, *57(18)*, 5141. doi: 10.1364/ao.57.005141.
15. Markschies, C.; Buckhout, T.; Elsässer, T.; Huber, G.; Klopp, P.; New Yb^{+3} - doped laser materials and their application in continuous-wave and mode-locked lasers, **2006**, 12 44-56
16. Jafari, A. K.; Aas, M.; Continuous-wave theory of Yb:YAG end pumped thin-disk lasers **2009**, *23*, 45-55
17. Petermann, K.; Highly Yb-doped oxides for thin-disc lasers, *Journal of Crystal Growth* **2005**, *275(1–2)*, 135–140. doi: 10.1016/j.jcrysgro.2004.10.077.
18. Katz, M.; Introduction to geometrical optics, *World Scientific Publishing Co. Pte. Ltd. Singapore* **2002,** *23*, 23-34
19. Maksutov, D. D.; *Newcatadioptric meniscus system, JOSA*, **1984,** 34, 270.
20. Kinzer, P. E.; Stargazing Basics Getting Started in Recreational Astronomy, *Cambridge University Press* . **2015**, *12*, 43-55
21. Mullaney, J.; *A Buyer's and User's Guide to Astronomical Telescopes & Binoculars*. **2007**. 46. ISBN 9781846287077.
22. Baril, M. R.; A photovisual Maksutov Cassegrain telescope". Although convenient, this design is limited to focal ratios above *f*/15 unless an aspheric correction is applied to some element in the optical system. **2005**, *34*, 55-67
23. Gross, H.; Fritz, B.; Bertram, A.; Telescopes. Handbook of Optical Systems*: Survey of Optical Instruments* . **2008,** *4*, 723-864.
24. H. Y.; Al Hammod, Design And Analysisa Zoom Cassegrain Telescope Cover Middle Ir Region Using Zemax Program, **2017,** *6, 8*, 178–185,
25. Kamus, S. F.; Lipin, N. A.; Sokolskii, M. N.; Levandovskaya, L. E.; Denisenko, S. A.; "Amateur telescopes," *J. Opt. Technol*. **2002**, *69*, 671-688
26. Shwayyea, A. K.; Hasan, A. B. Simulation and Evaluation of a Variable Effective Focal Length of Refractive Binocular Telescope. *Ibn Al-Haitham Journal for Pure and Applied Sciences.* **2022,** *35*,*3*,65-75.
27. Mullaney, J.; A Buyer's and User's Guide to Astronomical Telescopes and Binoculars. *Springer*. **2007,** *33*, 56-76
28. Baril, M. R.*;* A photovisual Maksutov Cassegrain telescope. *Archived from* the original. **2006,** *10.* 29-38.
29. Karp, J.International Telecommunication Union (ITU), *Optical System design and Engineering Consideration*, **2016,** *12*, 78- 88
30. K.; Miyamoto, Image Evaluation by Spot Diagram Using A Computer, *Appl. Opt.* **1963**, *2*,1247-1250.